Heliyon 7 (2021) e06969

Contents lists available at ScienceDirect

Heliyon

journal homepage: www.cell.com/heliyon

Research article

New approach for the dimensionless analysis of a unidirectional flow solar reactor based on Damköhler's number profiles

Héctor L. Otálvaro-Marín [a,b,c,*], Fiderman Machuca-Martínez [a]

[a] Escuela de Ingenieria Química, Universidad del Valle, A.A. 25360, Cali, Colombia
[b] MADE Group, Food Engineering Program, Universidad de la Amazonia, Florencia, Colombia
[c] IDEI Group, I+D Educación e Ingeniería, Cali, Colombia

ARTICLE INFO

Keywords:
Photoreactor
Tubular reactor
Scaling-up
Reactor design
Modeling
Finite differences

ABSTRACT

A methodology for the analysis of the behavior of complex reactors based on the construction of profiles of a dimensionless number (Damköhler) for each main chemical species (Da_i) was proposed. A 4-chlorophenol mineralization reaction in a heterogeneous solar reactor with suspended TiO_2 and addition of H_2O_2 with tubular geometry and radiation collectors, fluid flow and a recirculation system was selected as a complex model system in order to validate the approach. The dynamic behavior of the reactor in dimensionless variables was modeled as a function of Da_i. Where $Da_i(z,t)$ is a local property and grouped the optical and surface's properties of the catalyst, catalyst load, radiation intensity, the photon absorption rate, rate of non-photochemical reactions, the H_2O_2 effect, the reaction rate of different stages like adsorption, attack of radicals, surface reactions, plus design and operation variables like reactor volume and volumetric flow.

A coupling of orthogonal collocation and Runge-Kutta methods were used to solve the PDEs and carry out the simulations to the different experimental conditions, resulting in profiles of Da_i, C_i, and conversion in function of time and space. The Da_i profiles proposed in the new methodology are capable of describing the disturbances in solar reactors, to indicate consumption and generation rates, instantaneous changes of reaction rate, to describe competitive reactions and quenching effects and to determine equilibrium concentrations, all of the above at each time and space. Therefore, this approach is a analysis tool of reactors which complements the concentration profile. This methodology can be extended to other reactive systems, adapting the intrinsic reaction rates.

1. Introduction

Simulation has been widely used to describe complex systems, such as reactors, in order to design new geometries, determine the volume of new reactors, analyze different scenarios, determine the conversion and optimize operating variables [1, 2, 3]. Solar reactors are used in water treatment research to degrade pollutants by advanced oxidation process. These reactors can be heterogeneous with semiconductors suspended in a solution, they do not have a uniform distribution of radiant energy [4], in addition the radiation fluctuates at every moment, modifying the local rates of the reactions [5]. The tubular reactor with compound parabolic collectors CPCR [6] redirects the surrounding radiation to a tube with high transmittance walls [7]. In a sufficiently long tubular reactor, and with turbulent flow conditions ($Re > 1700$) [8], the flow can be considered to vary mainly in one direction only, and it can be classified as a unidirectional flow reactor. This reactor has been selected as a model reactor of a complex behavior.

A mathematical expression for the kinetic rate (r) of 4-chlorophenol mineralization for a simplified reaction mechanism of 29 elemental stages was described for the TiO_2/H_2O_2 system with solar radiation [9]. The main chemical species whose kinetic rates were determined are hydrogen peroxide and total organic carbon. The 4-chlorophenol mineralization by solar photocatalysis with TiO_2 and hydrogen peroxide was selected as a complex reaction model in order to apply the new approach for reactor analysis.

The dimensionless continuity equation as a function of the Damköhler's number (Da) for a reaction that follows a kinetic given by a n-th power law in unidirectional flow reactors was reported as $\partial \overline{C}_A/\partial \overline{t} = -\partial \overline{C}_A/\partial \overline{z} - \overline{C}_A^n Da_{A,inlet}$ [10], where Da is the ratio of the reaction rate to the global movement rate of the fluid, or alternatively, the product

* Corresponding author at: Escuela de Ingenieria Química, Universidad del Valle, A.A. 25360, Cali, Colombia.
E-mail address: hector.otalvaro@correounivalle.edu.co (H.L. Otálvaro-Marín).

https://doi.org/10.1016/j.heliyon.2021.e06969
Received 20 January 2021; Received in revised form 14 March 2021; Accepted 27 April 2021

of the reaction rate and the residence time. Then, to the inlet conditions: $Da_{A,inlet} = -r_{A,inlet}\tau_R/C_{A,initial}$. The solution of profiles of C_A and $Da_{A,inlet}$ in function of time and space, were useful for the design and simulation of these reactors. However, many kinetic rates are more complex and can experience fluctuations, as is the case of solar reactors. The general expression for any kinetic expression with multiple reactive species was reported as $\partial\overline{C}_i/\partial\overline{t} = -\partial\overline{C}_i/\partial\overline{z} - Da_i(z,t)$ [10], where Da_i is a function of space and time $Da_i = -r_i(z,t)\tau_R/C_{i,initial}$. Generating one partial differential equation (PDE) for each i-species.

There are different methods for solving PDEs. For example, a study [11] on numerical analysis of the behavior of a homogeneous tubular reactor in which a cubic autocatalytic reaction is coupled to diffusion and convection transport described concentration profiles obtained by numerical solution using the finite element, orthogonal collocation and finite difference method. An industrial reactor was simulated by solving its PDEs with two spatial variables and one temporal using the method of lines (MOL) in order to generate concentration, conversion and temperature profiles [12]. These numerical methods use space discretization to transform the PDEs system into a larger ODEs system. On the other hand, autocatalytic reactions have been modeled by the Brusselator model and their solution was obtained by the Adomiam decomposition method (ADM) deriving exact analytical solutions and by obtaining analytical approximations with a high degree of accuracy [13]. The techniques to solve a PDEs system are numerous [14] and we exemplify only one particular technique in this study (orthogonal collocation + ODEs solver). We will focus mainly on the modeling that leads to the desired dimensionless numbers in this study and the construction of their profiles for a detailed analysis of the reactor rather than the resolution methodology of PDEs, which can be modified to taste.

This study aims to indicate how to build the profiles of the Damköhler number of the main chemical species and show the usefulness of these in the analysis of complex reactors, taking as a model the mineralization of 4 chlorophenol in a solar tubular reactor.

2. Methodology

2.1. New approach for the analysis of the behavior of reactors

The authors propose the construction of Damköhler number profiles for each main reactive chemical species for the analysis of reactors and complex reactions as follows. Starting from the mass conservation equation for a continuous medium, the simplifications that can be assumed in the reactor are applied to generate a simplified continuity equation (Fig. 1). On the other hand, on the reaction mechanism, considerations of the rates are made in each stage and a mathematical expression is constructed for the intrinsic reaction rate. This is replaced in the simplified continuity equation to obtain the reactor design equation. Fig. 1 describes the new proposal for reactor analysis by introducing a Damköhler number for each main species.

In order to illustrate the new methodology applied to a reactor and complex reactions, the tubular solar reactor described in [9] was selected. It considers complex operation conditions, and even perturbations in time. The mineralization of 4-chlorophenol by heterogeneous photocatalysis with suspended TiO_2 assisted with hydrogen peroxide carried out in the previous reactor was selected as a model reaction to illustrate the methodology.

The mathematical expression for the intrinsic reaction rates were reported in [9] and the simplified continuity equation of the reactor was derived in [10]. These results are collected before continuing with the methodology as indicated in Fig. 1.

2.2. Dimensionless reactor design equation

The approach is based on the adimensionalization of the partial differential equation of continuity by species expressed as a function of the Damköhler number Da_i, where it is variable in time and space.

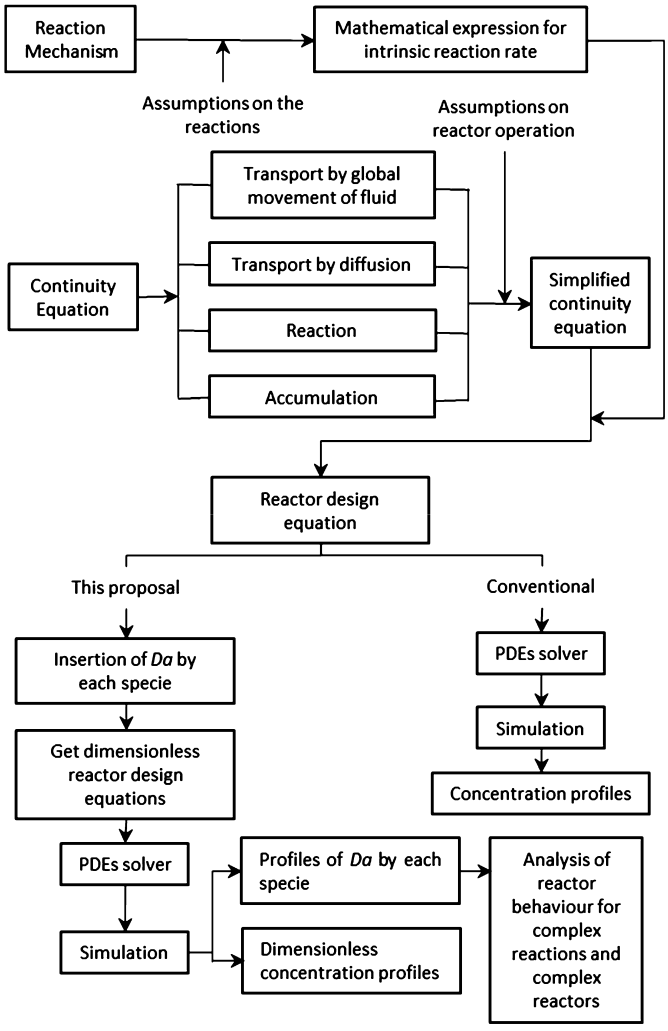

Fig. 1. Scheme of the methodology of mathematical modeling, simulation and design of reactors in general and the new approach for the analysis of reactor behavior.

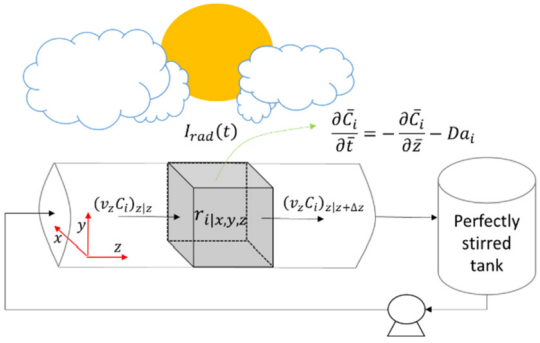

Fig. 2. Diagram of the dynamic reactive system.

Fig. 2 shows a schematic of the reactor in a recycle system. The reactor is tubular with compound parabolic collectors CPCR, connected to a recirculation tank and a feed pump to the reactor.

The following assumptions were taken into account. Let us consider a unidirectional flow reactor on z-coordinate, in transient state, with negligible diffusion, constant density and average velocity in z equal to v ($cm\,s^{-1}$). The design equation in dimensionless variables under this assumption is: $\partial\overline{C}_i/\partial\overline{t} = -\partial\overline{C}_i/\partial\overline{z} - Da_i$, see the derivation in [10]. For

total organic carbon (substance A) and H_2O_2 (substance B), the mass balance equations within the reactor are expressed as follows ($i = A, B$):

$$\frac{\partial \overline{C}_A}{\partial \overline{t}} = -\frac{\partial \overline{C}_A}{\partial \overline{z}} - Da_A(z,t) \tag{1}$$

$$\frac{\partial \overline{C}_B}{\partial \overline{t}} = -\frac{\partial \overline{C}_B}{\partial \overline{z}} - Da_B(z,t) \tag{2}$$

where dimensionless variables are defined as follows:

$$\overline{C}_i \equiv C_i / C_{i,0} \tag{3}$$

$$\overline{z} \equiv z / L_R \tag{4}$$

$$\overline{t} \equiv t / \tau_R \tag{5}$$

$$Da_i \equiv -r_i \tau_R / C_{i,0} \tag{6}$$

where overline variables and Da_i are dimensionless. C_i is the concentration of i-component (mol cm^{-3}); $C_{i,0}$ is the initial concentration of i-component (mol cm^{-3}); $\overline{C}_i$ is the dimensionless concentration of i-component; L_R is the reactor length (cm); z is the length on z-coordinate (cm); $\overline{z}$ is dimensionless z-coordinate; τ_R is the mean residence time inside the reactor (s); the mean residence time in a unidirectional flow reactor is L_R/v; $-r_i$ is the local intrinsic reaction rate of i (mol of i cm^{-3} s^{-1}); $Da_i(z,t)$ is the local Damköhler number of i-component (dimensionless); t is the time (s); $\overline{t}$ is dimensionless time.

Without H_2O_2 initial load ($C_{B,0} = 0$), then, the variables $\overline{C}_B$ and Da_B are redefined as $\overline{C}_B \equiv C_B / C_B^{Ref}$, and $Da_B \equiv -r_B \tau_R / C_B^{Ref}$, where C_B^{Ref} is an any reference value (mol cm^{-3}), the above does not affect it because the limiting substance is A, and the conversion of the system is measured with respect to A.

The boundary conditions for a perfectly mixed external tank without chemical reaction are:

$$\left.\frac{d\overline{C}_A}{d\overline{t}}\right|_{(\overline{z}=0)} = \frac{1}{\overline{\tau}_{TK}}\left(\overline{C}_{A(\overline{z}=1)} - \overline{C}_{A(\overline{z}=0)}\right) \tag{7}$$

$$\left.\frac{d\overline{C}_B}{d\overline{t}}\right|_{(\overline{z}=0)} = \frac{1}{\overline{\tau}_{TK}}\left(\overline{C}_{B(\overline{z}=1)} - \overline{C}_{B(\overline{z}=0)}\right) \tag{8}$$

where $\overline{\tau}_{TK}$ is the dimensionless residence time in the tank normalized between the residence time of the reactor, $\overline{\tau}_{TK} = \tau_{TK}/\tau_R$; $\overline{C}_{i(\overline{z}=0)}$ and $\overline{C}_{i(\overline{z}=1)}$ are the dimensionless concentrations of i-component at the inlet and outlet of the reactor respectively.

The initial conditions are:

$$\overline{C}_{A(\overline{t}=0)} = 1 \tag{9}$$

$$\overline{C}_{B(\overline{t}=0)} = \begin{cases} 1 & \text{with initial charge} \\ 0 & \text{without initial charge} \end{cases} \tag{10}$$

2.3. Damköhler in photocatalytic reactors

We will consider the particular case of the following study. The mineralization intrinsic kinetic rate of 4-chlorophenol (4-CP) in a photocatalytic reactor with suspended TiO_2 and H_2O_2 was validated for different geometries, substrates, operating conditions and solar radiation. The expressions for kinetic rates were obtained from a simplified set of 29 elemental reactions. Details of the proposed reaction mechanism and analytical deduction of kinetic expression can be found in [9]. For A and B the reaction rates are:

$$-r_A = \sqrt{C_{mp}} S_g k_{cat} \sqrt{I_a} Z Q_A \tag{11}$$

$$-r_B = \sqrt{C_{mp}} S_g k_{cat} W Z \sqrt{I_a} Q_B + S_g I_a \beta'_{HO\cdot} \left(\frac{Z}{F}\right)^2 \tag{12}$$

where

$$Q_A = \frac{\beta'_A}{F} \tag{13}$$

$$Q_B = \frac{\beta_B C_B}{F} \tag{14}$$

$$F = 1 + \beta_B C_B + \beta_{\mathrm{NOM}} C_{NOM,0} \tag{15}$$

$$Z = 1 + \alpha_2 C_B \tag{16}$$

$$W = 1 + (\alpha_2/\beta_B) F/Z \tag{17}$$

$$I_a = \langle LVRPA_{solar} \rangle_{Area} \tag{18}$$

where $-r_A$ is the photocatalytic kinetic rate of 4-CP mineralization (mol cm^{-3} s^{-1}); β'_A is the global kinetic constant of hydroxyl radical attack to 4-CP at zero-order reaction rate respect to total organic carbon (TOC) (dimensionless); C_{mp} is the mass concentration of catalyst (g cm^{-3}); S_g is the specific surface area of the catalyst (cm^2 g^{-1}); k_{cat} is an intrinsic constant of surface reactions involving hydroxyl radical generation, electron and hole capture, and recombination (mol$^{0.5}$ g$^{0.5}$ cm^{-2} s$^{-0.5}$); I_a is the average of local volumetric rate of photon absorption $LVRPA$ in the cross-section of the fluid flow (Einstein cm^{-3} s^{-1}); α_2 is the reaction constant of peroxide as an acceptor of photogenerated electrons (cm^3 mol^{-1}); C_B is the H_2O_2 molar concentration (M); $C_{NOM,0}$ is the initial concentration of natural organic matter NOM, different of 4-CP, measured as initial organic carbon (M); Q_A is the mineralization quenching by H_2O_2 and NOM; β_B and β_{NOM} are the adsorption and degradation global constant of H_2O_2 and NOM respectively. The value of the kinetic constants is [9]: $k_{cat} = 6.57 \times 10^{-8}$ mol g$^{0.5}$ cm^{-2} s$^{-0.5}$ Einstein$^{-0.5}$, $\alpha_2 = 0.127$ M^{-1}, $\beta'_{HO\cdot} = 1.219 \times 10^{-5}$ mol g cm^{-2} Einstein^{-1}, $\beta_B = 5.7508 \times 10^3$ M^{-1}, $\beta_{\mathrm{NOM}} = 16.88$ M^{-1}, and $\beta'_A = 5.71 \times 10^{-2}$ (dimensionless).

Replacing the photocatalytic reaction rate in Eq. (6), we express the Damköhler number for a photocatalytic reactor:

$$Da_A = \left(\sqrt{C_{mp}} S_g k_{cat} \sqrt{I_a} Z Q_A\right) \tau_R / C_{A,0} \tag{19}$$

$$Da_B = \left(\sqrt{C_{mp}} S_g k_{cat} \sqrt{I_a} Z W Q_B + S_g I_a \beta'_{HO\cdot} \left(\frac{Z}{F}\right)^2\right) \tau_R / C_{B,0} \tag{20}$$

The variable parameters Da_i grouped the optical and surface characteristics of the catalyst, catalyst load, instantaneous radiation intensity, the absorption rate of photons, rate of non-photochemical reactions, the effect of hydrogen peroxide, the rate of reactions of different stages like adsorption, attack of radicals, surface reactions, design variable like the reactor volume, and operation variable like volumetric flow. All the effects are grouped in a single dimensionless parameter which allows to study them for an analysis of the behavior of the reactor in a very easy and convenient way.

2.4. LVRPA at solar CPC reactor

Due to the simplification of the reactor as a unidirectional reactor, it is convenient to estimate the $LVRPA(x,y,z,t)$ as an average value in a cross section at distance z, $\langle LVRPA(z,t) \rangle_{Area}$.

For a solar reactor with a variable radiation intensity $G_{solar}(t)$, the $\langle LVRPA_{solar} \rangle_{Area}$ at any time is calculated based on a reference state as follows [5]:

$$\langle LVRPA_{solar} \rangle_{Area} = G_{solar}(t) \frac{\langle LVRPA_{Ref} \rangle_{Area}}{G_{Ref}} \tag{21}$$

where $\langle LVRPA_{Ref} \rangle_{Area}$ is the $\langle LVRPA \rangle_{Area}$ evaluated at a constant radiation intensity G_{Ref}. The estimation of $LVRPA_{Ref}(x,y,z)$ in a CPC reactor is complex, however, it has already been extensively investigated. Three models are grouped together: a ray-tracing model to track trajectories and incident energy at the reactor boundaries; the radiant boundary layer model to determine the photon penetration length and the radiant energy absorption-dispersion model to determine the absorbed energy profile along each path. Details are described in [5]. The Eq. (21) is suitable to calculate the intensity of radiation absorbed at any instant of time, this requires evaluating the $\langle LVRPA_{Ref} \rangle_{Area}$ only once and to have registered the oscillations of solar radiation with a radiometer.

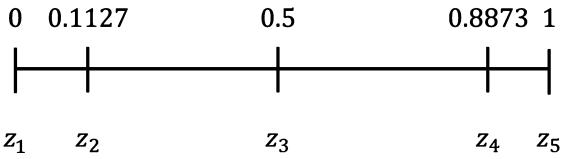

Fig. 3. Scheme of the normalized domain of reactor length.

2.5. Experimental conditions and chemical analysis

A recycling system was used with an external tank where the fluid is saturated with air. The tubular solar reactor with compound parabolic collectors CPCR has an irradiated area of 1.22 m^2, an arrangement of 10 borosilicate tubes, a total length of 1220 cm and an internal radius of 1.45 cm [6]. The mineralization of 4-chlorophenol (Merck), was measured in total organic carbon TOC analyzer, Shimadzu TOC-VCPH. Conditions: flow 332.5 cm^3/s, mean residence time in the reactor 24.2 s, mean residence time in the tank 66.2 s, catalyst load of TiO_2 Evonik P25 0.21 g/L, initial TOC concentration 1.32×10^{-6} mol of C/cm^3 (28.3 ppm of 4-chlorophenol), natural organic matter NOM present in the water of the pilot experiment (30 L) 3.6167×10^{-7} mol of C/cm^3. The radiant flux was recorded using a Delta Ohm with UV-A probe (315-400 nm) and the radiant flux between 280 and 315 nm was calculated using a ratio of areas: one (1) under the radiation intensity curve of the Simple Model of the Atmospheric Radiative Transfer of Sunshine, SMARTS [15] and the other area under the curve of the integration of radiation in the UV-A region recorded experimentally [9].

The total organic carbon (TOC) was measured in a Shimadzu TOC-VCPH Organic Carbon Analyzer with a non-dispersive infrared detector. The H_2O_2 concentration was measured by spectrophotometric measurement of the yellow color intensity in H_2O_2 solutions treated with a titanium sulfate reagent, which was proposed by Eisenberg in 1943 [16] and modified by Barona [17].

2.6. Ortogonal collocation method

The coupled system of PDEs (Eqs. (1) and (2)) can be solved using different methods: finite differences, method of lines MOL [18], orthogonal collocation method, among others. For the mentioned methods it is possible to discretize the spatial variable and keep the temporal variable as continuous. The orthogonal collocation method was selected because it makes an approximation of the solution using a discretization of the space (reactor length) in only 5 points.

The orthogonal collocation method [19] was applied to transform the problem of solving two partial differential equation (PDE) for solving a system of ten ordinary differential equations (ODEs).

The reactor length is divided into orthogonal points (Fig. 3), where z is normalized $\overline{z}=z/L_R$. Each point is understood as a node within the orthogonal collocation method.

Let to define $\overline{C}_{i,m}\equiv\overline{C}_i(\overline{z}=z_m,\bar{t})$ with $m=1,2,3,4,5$.

The PDEs (1) and (2), and the boundary conditions (7) and (8) are rewritten as the following system of ODEs:

$$\frac{d\overline{C}_{A,1}}{d\bar{t}}=\frac{1}{\overline{\tau}_{TK}}\left(\overline{C}_{A,5}-\overline{C}_{A,1}\right) \tag{22}$$

$$\frac{d\overline{C}_{A,2}}{d\bar{t}}=-s^{(2)T}\overrightarrow{C_A}-Da_{A,2} \tag{23}$$

$$\frac{d\overline{C}_{A,3}}{d\bar{t}}=-s^{(3)T}\overrightarrow{C_A}-Da_{A,3} \tag{24}$$

$$\frac{d\overline{C}_{A,4}}{d\bar{t}}=-s^{(4)T}\overrightarrow{C_A}-Da_{A,4} \tag{25}$$

$$\frac{d\overline{C}_{A,5}}{d\bar{t}}=-s^{(5)T}\overrightarrow{C_A}-Da_{A,5} \tag{26}$$

$$\frac{d\overline{C}_{B,1}}{d\bar{t}}=\frac{1}{\overline{\tau}_{TK}}\left(\overline{C}_{B,5}-\overline{C}_{B,1}\right) \tag{27}$$

$$\frac{d\overline{C}_{B,2}}{d\bar{t}}=-s^{(2)T}\overrightarrow{C_B}-Da_{B,2} \tag{28}$$

$$\frac{d\overline{C}_{B,3}}{d\bar{t}}=-s^{(3)T}\overrightarrow{C_B}-Da_{B,3} \tag{29}$$

$$\frac{d\overline{C}_{B,4}}{d\bar{t}}=-s^{(4)T}\overrightarrow{C_B}-Da_{B,4} \tag{30}$$

$$\frac{d\overline{C}_{B,5}}{d\bar{t}}=-s^{(5)T}\overrightarrow{C_B}-Da_{B,5} \tag{31}$$

with the initial condition for all points:

$$\overline{C}_{A,m(\bar{t}=0)}=1 \tag{32}$$

$$\overline{C}_{B,m(\bar{t}=0)}=\begin{cases}1 & \text{with initial charge}\\ 0 & \text{without initial charge}\end{cases} \tag{33}$$

where $Da_{i,m}\equiv Da_i\left(z_m,\bar{t}\right)$ for $i=A,B$; for $m=1,2,3,4,5$. At Eqs. (22)–(31), the $\vec{C}_i$ is the dimensionless concentration vector of the ith-component at all orthogonal points and S is the matrix of the orthogonal collocation method containing the coefficients of the first order derivative. Note that the spatial derivative at a point z_m is a function of the concentration at all orthogonal points. The $\vec{C}_i$ vector and the matrix of the first derivatives $\overline{\overline{S}}$ are respectively:

$$\vec{C}_i=\begin{bmatrix}\overline{C}_{i,1}\\ \overline{C}_{i,2}\\ \overline{C}_{i,3}\\ \overline{C}_{i,4}\\ \overline{C}_{i,5}\end{bmatrix} \tag{34}$$

$$\overline{\overline{S}}=\begin{bmatrix}s^{(1)T}\\ s^{(2)T}\\ s^{(3)T}\\ s^{(4)T}\\ s^{(5)T}\end{bmatrix}=\begin{bmatrix}-13.00 & 14.79 & -2.67 & 1.88 & -1.00\\ -5.32 & 3.87 & 2.07 & -1.29 & 0.68\\ 1.50 & -3.23 & 0.00 & 3.23 & -1.50\\ -0.68 & 1.29 & -2.07 & -3.87 & 5.32\\ 1.00 & -1.88 & 2.67 & -14.79 & 13.00\end{bmatrix} \tag{35}$$

The system of 10 ordinary differential equations, Eqs. (22)–(31), is solved using the fourth order Runge Kutta method. Alternatively, the as-built adaptive Runge Kutta (4,5) procedure in MATLAB Software named as “ode45” can be used.

3. Results and discussion

Figs. 4, 5, 6 and 7 show the dynamic profiles of the reactor variables during the mineralization of 4-chlorophenol in a tubular CPC reactor (unidirectional flow reactor) on a sunny day with fluctuations in radiation intensity. 30 L were treated with an initial concentration of total organic carbon (component A) from the organic pollutant equal to 2.82×10^{-6} mol de C/cm^3 (33.9 ppm) with an initial hydrogen peroxide load (component B) equal to 3.00×10^{-6} mol/cm^3 (102.3 ppm) and a total organic carbon from natural organic matter (NOM) of the treatment water of 4.34×10^{-7} mol de C/cm^3. These values in units of mol/cm^3 correspond to the initial conditions and are also used in the definitions of Da_A and Da_B. The Figures are presented in dimensionless time $\bar{t}=t/\tau_R$, where the mean residence time in the reactor was 24.57 s.

$Da_i(z,t)$ profile of the main species

Fig. 4 shows the dimensionless solar radiation intensity referred to 24 W/m^2 (I_0) varying in time. It was calculated as the cumulative irradiation measured during a time interval in between. On the right vertical axis, the Da_A is shown at each node within the reactor varying in time.

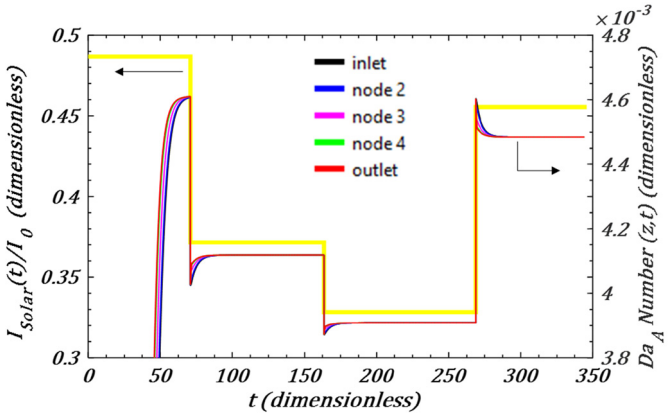

Fig. 4. Da_A profile and radiation intensity as a function of time between the residence time of the reactor. The $Da_A(z,t)$ is shown for nodes located along the z-axis according to Fig. 2.

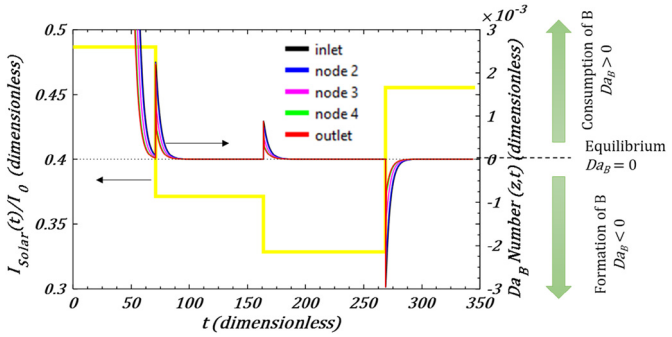

Fig. 5. Da_B profile and radiation intensity as a function of time between the residence time of the reactor. The $Da_B(z,t)$ is shown for nodes located along the z-axis.

The radiation intensity fluctuated with average values in intervals from 7.9 W/m^2 to 11.7 W/m^2. Instantaneous changes in radiation caused a pronounced variation in the Da_A at any point within the reactor. A study showed that an intrinsic mineralization kinetic, with explicit photon absorption effect can satisfactorily describe the reactor on sunny and cloudy days [6]. This result is consistent with the models and methods used.

The Da_A increased in the first time interval at constant solar radiation intensity. Based on these and other simulation observations of the model, it is concluded that Da_A depends on the concentration of components A, B and strongly on the instantaneous radiation intensity:

$$Da_A = f_1\left(C_A, C_B, I_{Solar}\right) \tag{36}$$

Fig. 5 shows the Da_B as a function of time for each node on the right vertical axis. The radiation intensity was also plotted to appreciate its effect on Da_B. As well as Da_A a pronounced effect is evidenced for a sudden change in intensity of solar radiation:

$$Da_B = f_2\left(C_A, C_B, I_{Solar}\right) \tag{37}$$

The C_A, C_B and I_{Solar} are strongly interrelated and depend on z and t, and both continuity equations should be simultaneously solved:

$$\frac{\partial \overline{C}_A}{\partial \overline{t}} = -\frac{\partial \overline{C}_A}{\partial \overline{z}} - Da_A\left(C_A, C_B, I_{Solar}\right) \tag{38}$$

$$\frac{\partial \overline{C}_B}{\partial \overline{t}} = -\frac{\partial \overline{C}_B}{\partial \overline{z}} - Da_B\left(C_A, C_B, I_{Solar}\right) \tag{39}$$

$$I_{Solar} = f_3(t) \tag{40}$$

This conclusion can be reached based on the reaction rates of the species, however, it is necessary to generate the profiles of Da_A and Da_B in z and t in order to determine possible simplifications on the reaction rates, appreciate the effect of the intensity of solar radiation, identify the main chemical reactions that control the reactor in a given time and space, chemical equilibria, formation and consumption of species as will be discussed in the following sections.

Rigorous kinetic models for the degradation of 4-chlorophenol in laboratory and bench scale reactors with recirculation and irradiated with lamps were described [20]. Intrinsic reaction rates described the dependence with the LVRPA, 4-chlorophenol concentration, and main intermediates of degradation by coupled differential equations. The reported kinetic parameters are not comparable with this study, since they describe the degradation, and this study describes the mineralization. However, there are similar dependencies.

The proposed methodology for the analysis of the reactive system makes explicit the effect of a sudden change in intensity of solar radiation on the Da_i instantaneously.

Relative rates of hydroxyl radical attack

We will analyze the first time interval at constant solar radiation intensity. Initially, the reactor was charged with H_2O_2. At initial conditions the Da_A had a minimum value of 3.19×10^{-4} increasing to a maximum value of 4.61×10^{-3} in the first time interval (Fig. 4). Meanwhile, Da_B at the initial conditions is maximum with 9.06×10^{-2} and rapidly decays to 2.54×10^{-5} in the same time (Fig. 5). Both Da_A and Da_B are positive, therefore the consumption of them occurs simultaneously and competitively to react with the hydroxyl radicals, discussed by [21, 22]:

$$HO^{\bullet} + H_2O_2 \longrightarrow H_2O + HO_2^{\bullet}$$

$$HO^{\bullet} + R_i \longrightarrow R_j$$

$$HO^{\bullet} + NOM \longrightarrow R_j$$

where R_i represents an organic substrate, R_j represent degradation by-products and NOM is the natural organic matter present in the treatment water.

Furthermore, following Le Châtelier's principle, in excess of H_2O_2, the consumption of H_2O_2 is favored by the following reaction:

$$Ti^{IV} - H_2O_2 + e^- \rightleftharpoons Ti^{IV} - HO^{\bullet} + OH^-$$

The high Da_B at the beginning of the reaction indicates a high rate of consumption of B, that decreases as B is consumed, and simultaneously increases the degradation reaction of A by radical attack, increasing the Da_A. This dynamic relationship results in a complex system. Also, there are related adsorption stages on the surface that are considered in equilibrium because they occur very quickly, and are taken into account in the kinetic model [9].

The methodology established a complex dynamic relationship between the Damköhler number of the species, characterized by its complex reaction mechanism. The Damköhler numbers of the species can be used to identify when the reactions favor the formation or consumption of H_2O_2 by the hydroxyl radical according to the sign of Da_B, and quantify it by its magnitude as a dimensionless parameter. The reaction rate profiles are commonly described with dependence on its units [23, 24], being less suitable for an reactor analysis respect to one based on the dimensionless Da_i.

Effect of radiation fluctuation

The reaction rate of A explicitly leads to $Da_A \propto \sqrt{I_{Solar}}$, consistent with [6, 25], it explains the changes of Da_A in the event of sudden changes on the radiation intensity in the Fig. 4:

$$\frac{Da_{A1}}{Da_{A2}} = \left(\frac{I_{Solar1}}{I_{Solar2}}\right)^{0.5} \tag{41}$$

In contrast, the relationship between radiation intensity and Da_B is not simple. A sudden decrease in radiation intensity increases Da_B, accelerating the consumption rate of B. On the contrary, a sudden increase in radiation intensity generates high negative values of Da_B, so, it accelerates the formation rate of B.

Here the reactions of consumption and formation of B play an important and complex role. On the one hand, the formation of B is due to the increase in the intensity of solar radiation, as show the Fig. 4, then, the produced holes and HO• radicals increase and the last ones react to form H_2O_2 [21, 22]:

$$TiO_2 + h\nu \overset{\Phi_{TiO_2}\kappa}{\rightleftharpoons} e^- + h^+$$

$$\mathrm{Ti^{IV} - OH^- + h^+ \rightleftharpoons Ti^{IV} - HO^\bullet}$$

$$\mathrm{HO^\bullet + HO^\bullet \longrightarrow H_2O_2}$$

On the other hand, a steady state is disturbed by the sudden decrease in radiation intensity. The concentration of hydroxyl radicals (it was estimated from an equilibrium with the radiation intensity) decreases instantly, and the rate of formation becomes slower than that of consumption of B, therefore, the net reaction rate is consumption by B:

$$\mathrm{Ti^{IV} - H_2O_2 + e^- \rightleftharpoons Ti^{IV} - HO^\bullet + OH^-}$$

$$\mathrm{HO^\bullet + H_2O_2 \longrightarrow H_2O + HO_2^\bullet}$$

Chemical equilibrium

The above reactions are dynamic and fast. In the Fig. 5 constant segments of Da_B are equal to zero, here the rates of formation and consumption of B have been equalized and the concentrations of the species of the reactions involved reach their equilibrium concentration. These equilibria are disturbed by radiation intensity, producing a new equilibrium concentration of B. An increase in radiation intensity produces a higher concentration of radicals and a higher concentration of B at equilibrium.

$$K_{Eq} = \frac{\left[\mathrm{H_2O_2}\right]_{Eq}}{\left[\mathrm{HO^\bullet}\left(G_{Solar}\right)\right]_{Eq}} \tag{42}$$

The profile of Da_B in the time allowed to identify consumption, equilibrium and formation of B during the reaction. Substance A is always consumed, consistent with a mineralization reaction.

The sign of Da_i indicates consumption, formation or equilibrium of species for positive, negative and zero values respectively. The magnitude of Da_i is a measure of the rate of each of these reactions.

The analysis made previously is at least difficult to conclude from the concentration profiles, which makes the profiles of the Damköhler number of the species a complementary tool for the analysis and compression of the reactive system. For all the above, the Damköhler number profiles are a tool for the analysis of complex reactors that complement the well-known concentration profiles.

Dimensionless concentration profiles

Fig. 6 shows the dimensionless concentration profiles of A and B over time at each node. The experimental data is presented in black diamonds and red squares for A and B respectively.

The $\overline{C}_A(z,t)$ y $\overline{C}_B(z,t)$ are shown for nodes located along the z-axis. The black and red marks represent experimental data of concentration of A and B respectively.

The zoom-up in Fig. 6 shows the concentrations of H_2O_2 in equilibrium that were obtained in the reaction for different intensities of radiation. In chronological order they were: 1.54, 1.37, 1.30 and 1.50 ppm of H_2O_2.

The kinetic rates of the reported mathematical model were used exclusively for simulation. The reported and adjusted model has a standard deviation of 1.30 ppm [9]. This is an acceptable fit to the experimental data.

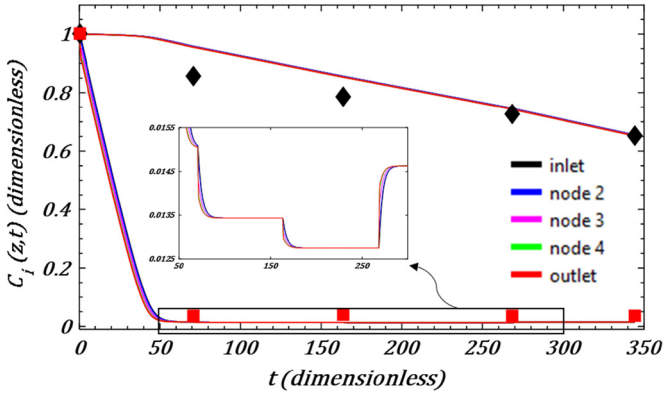

Fig. 6. Profile of 4-chlorophenol mineralization in a solar tubular unidirectional reactor.

Quenching

The concentration of A in Fig. 6 starts with a very small slope, which indicates negligible degradation of A at the start of the reaction. The concentration profiles allow to appreciate quenching effects on the degradation of A by initial excess of B [26], as expressed by the term Q_A of the reaction rate of A [9]:

$$Q_A = \frac{k_A C_A}{\alpha + k_A C_A + k_B C_B + k_{NOM} C_{NOM,0}} \tag{43}$$

For a load in excess of H_2O_2, the denominator is high and decreases as B is consumed. Q_A, $-r_A$ and Da_A are initially low and they increase progressively. The rate with which these events occur depends on the apparent reaction constants α, k_A, k_B, k_{NOM} which include rate constants of the hydroxyl radical attack steps described above, and of the adsorption steps on the surface [9]:

$$HO^\bullet + Ti^{IV} \overset{K_{HO^\bullet}}{\rightleftharpoons} Ti^{IV} - HO^\bullet$$

$$Site + A \overset{K_A}{\rightleftharpoons} A,ads$$

$$Ti^{IV} + H_2O_2 \overset{K_{H_2O_2}}{\rightleftharpoons} Ti^{IV} - H_2O_2$$

$$Site + NOM \overset{K_{NOM}}{\rightleftharpoons} Ti^{IV} - NOM$$

These reactions were assumed to be fast enough to be described at any moment by equilibrium.

In conclusion, Da_A includes the quenching effects due to the adsorption and hydroxyl radical attacks described by complex expressions of reaction rate. Likewise, this approach can be extended to Langmuir Hinshelwood or other kinetic rates.

Interpretation of Da_A

The variable parameter Da_A groups together the effects of the optical and surface properties of the catalyst, the load of the catalyst, the intensity of radiation fed to the system, the rate of absorption of photons by the catalyst, the effect of hydrogen peroxide, the rate of reactions of different stages and design variables, geometry and flow grouped in the mean residence time in the reactor, and the initial concentration of the system:

$$Da_A = \sqrt{C_{mp}} S_g k_{cat} \sqrt{LV\,RPA}\left(1 + \alpha_2\left[\mathrm{H_2O_2}\right]\right) Q_A \tau_R / C_A^0 \tag{44}$$

The term $\sqrt{C_{mp}} S_g k_{cat}$ is exclusive of the catalyst effect. A higher specific surface area S_g increases the adsorption rate on TiO_2 surface [27]. k_{cat} relates hydroxyl radical formation, electron-hole pair formation and recombination, all these reactions are charge transfer reactions that occur on the catalyst surface:

$$\mathrm{Ti^{IV} - OH^- + h^+ \rightleftharpoons Ti^{IV} - HO^\bullet}$$

$$\mathrm{Ti^{IV} - H_2O + h^+ \rightleftharpoons Ti^{IV} - HO^\bullet + H^+}$$

$$e^- + h^+ \longrightarrow \text{heat}$$
$$TiO_2 + h\nu \overset{\Phi_{TiO_2}\kappa}{\rightleftharpoons} e^- + h^+$$

A high k_{cat} indicates efficiency of surface reactions. k_{cat} and S_g can be modified by catalyst synthesis [28]. The C_{mp} increases $\sqrt{C_{mp}}$, but an excess presents a limitation on the transport and absorption of photons inside the reactor [29], affecting Da_A.

The effect of H_2O_2 is a matter of discussion because it accelerates competitive reactions while improving the capture of photogenerated electrons [21]:

$$Ti^{IV} - H_2O_2 + e^- \rightleftharpoons Ti^{IV} - HO^{\bullet} + OH^-$$

Natural organic matter (NOM) reacts with hydroxyl radicals and quenches the reaction [26] as expressed by quenching Q_A, Eqs. (13) and (15). Ultra clean water from laboratory removes the NOM, however, in a real case of water treatment it is mandatory to consider the limitation of the reaction by NOM.

Therefore, all the researchers who work in the area of photocatalysis from different specific fields are directly working to improve the Da_A, either from the synthesis of catalysts [30], modification of catalysts, broadening the spectrum of absorption [31], reactor geometry [32, 33], hydrodynamics of reactors and CFD [3], design of new reactors such as microreactors [34], development of new applications, or evaluation of other contaminants and mixtures. This parameter (Da_A) becomes a key element in the development of technology.

Design volume and solar or artificial light Intensity

The improvement of technology for use in treatment of higher flows requires increases of one or several orders of Da_A magnitude. Since $Da_A \propto \sqrt{I_{source}}$ where I_{source} can be natural or artificial, an increase of one or two orders of magnitude in the Da_A will require an increase in the I_{source} of 100 and 10^4 times respectively. Then, increasing the radiation intensity as an alternative to increase Da_A becomes unfeasible. This is a technical and economic problem in the photoreactor design.

On the contrary, Da_A is proportional to the mean residence time. This variable is easy to control by modifying the operating flow, estimating the new design volume of a reactor, or both, ensuring a fully developed turbulent flow to suspend the TiO_2 [35]. Also, it is possible to add baffles or longer fluid path through tubes [3, 33]. A lower volumetric flow Q increases both the mean residence time and Da_A. An interesting limiting case is when a batch reactor is used, the average residence time is equal to the duration of the operation and it can be increased several orders of magnitude for artificial radiation.

Therefore, to improve the performance of the reactor in a scaling-up of the technology for the treatment of higher flows, the operating volumetric flow can be modified, a design volume of the reactor can be estimated or the radiation source can be varied according to:

$$Da_A \propto V_{design}\sqrt{I_{source}}/Q \tag{45}$$

For the scaling-up of the reactor, a constant Da_A must be guaranteed (Eq. (45)), in order to keep the conversion.

When applying dimensionless variables to the system, the (absolute) variables of design, operation and reaction rate are grouped within Da_A and the external recirculation circuit in the boundary condition. This result is general for any reaction in a unidirectional flow reactor, even for systems described with variable Da. Due to these characteristics, this dimensionless design equation methodology can be extended to other reactive systems by redefining the specific expression for Da.

Relationship between Damköhler and conversion

Figs. 7a-c show the dynamic variables during 4-Chlorophenol mineralization and simulated and experimental conversion (X). Figs. 7a and 7b are experiments without an initial load of B, with (1.32 and 2.77) $\times 10^{-6}$ initial mol of C/cm^3; $\tau_R = 24.24$ s, 24.57 s and NOM of (3.71 and 3.23) $\times 10^{-7}$ initial mol of C/cm^3 respectively. The run in Fig. 7c

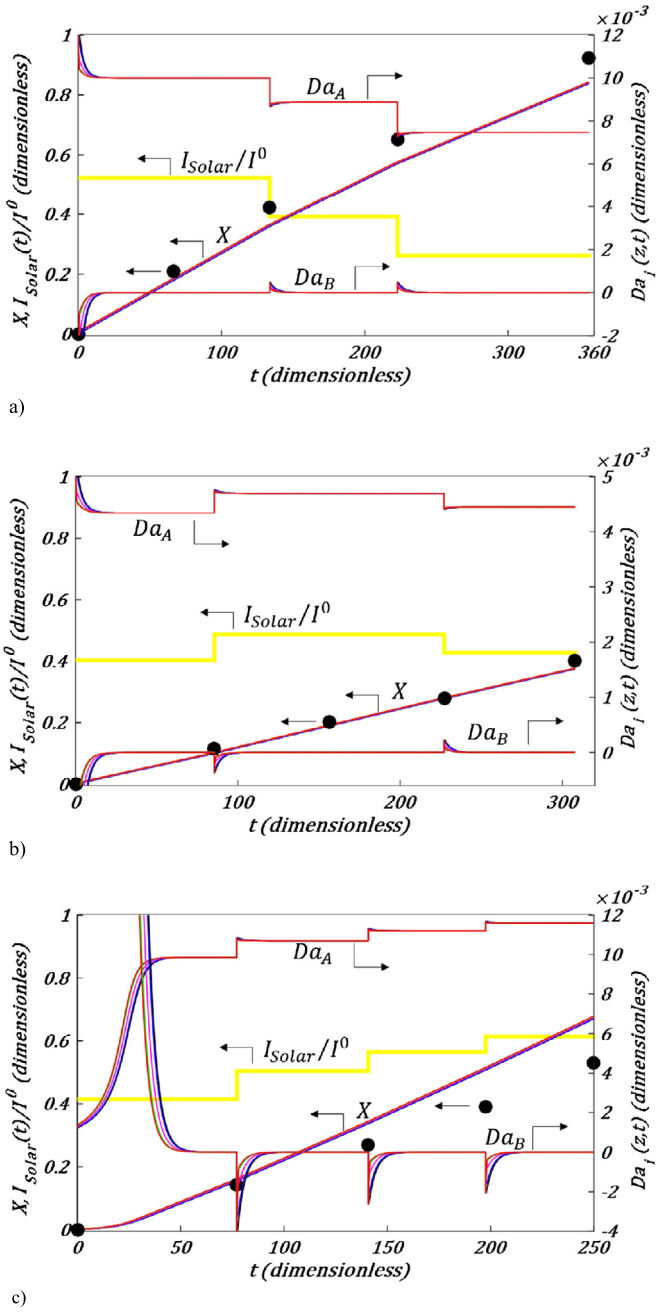

Fig. 7. Conversion (X) as a function of dynamic variables in the mineralization of 4-chlorophenol at different radiation and operating conditions. A) no initial charge of B, with 15.85 ppm of A, b) no initial charge of B, with 33.3 ppm of A, c) initial charge of B of 52.38 ppm, with 15.97 ppm of A. The black circles represent the experimental conversion.

has an initial charge of B of 1.54×10^{-6} mol of B/cm^3, with 1.33×10^{-6} mol of C/cm^3 from A, 4.24×10^{-7} initial mol of C/cm^3 from NOM and $\tau_R = 26.42$ s. Each run was performed on different days, with radiation intensities as illustrated in the yellow lines. The black circles are experimental data of the conversion taken from samples at the outlet of the reactor. The Damköhler numbers Da_A and Da_B are read from the right vertical axis, all other variables are read from the left.

Although the variables are dynamic in time and describe a complex system, mathematically, it can be seen that the highest conversion was obtained for the highest Da_A, higher time of integration on the partial differential equations that describe the changes in concentration in the reactor. In practical terms, the highest conversion is obtained at a higher

reaction rate, longer mean residence time, lower initial concentration, and longer operating time.

The methodology suggests obtaining the profiles of Da_i, and conversion vs dimensionless time ($\bar{t}$). We appreciate that they allow a more complete analysis than the profile of reaction rates and concentrations vs time in dimensional variables. The methodology can be extended to more than two main species.

4. Conclusions

A new approach to the analysis of the behavior of reactors was proposed and validated for a model reaction. The novelty of this work is based on the formulation of reactor modeling in local dimensionless numbers that group all the operating conditions, catalyst characteristics, reaction rates for a mechanism with photochemical and chemical reactions.

The proposed approach is based on a local dimensionless number as a function of time for each main chemical species (Damköhler's number, Da_i). This parameter is present in the dimensionless continuity equations that describe the transient behavior of the reactor. The dimensionless profiles presented by the approach allow an analysis that shows many advantages in respect to the modeling in dimensional variables. The conversion was determined as a function of the Da_i in a continuous tubular solar reactor as model reactor.

The parameter Da_i grouped together the effects of the optical and surface characteristics of the catalyst, catalyst load, fluctuating radiant flux, the rate of absorption of photons, the effect of hydrogen peroxide, the rate of reactions of different stages, and design and operation variables. This work proposed to graph the Da_i profiles vs dimensionless time as a tool for the analysis of the behavior of a complex reactor. The sign of Da_i of each species indicated formation, consumption or equilibrium concentrations with positive, negative and zero values respectively, and the magnitude indicated the dimensionless reaction rate.

The new approach allowed to analyze a complex dynamic system with competitive reactions, fluctuating radiation intensities, synergistic reaction, site adsorption, chemical and photochemical reaction in the reaction mechanism, quenching effects and photon transport.

For the scaling of the process, it was concluded that, it is possible to modify the operating volumetric flow, to estimate design volume of a new reactor or to modify the radiation source according to $Da_A \propto V_{design}\sqrt{I_{source}}/Q$, keeping Da_A and other conditions constant.

For the scaling-up of the process, it was concluded that, it is possible to modify the operating volumetric flow, to estimate the design volume of a new reactor or to modify the radiation source according to $Da_A \propto V_{design}\sqrt{I_{source}}/Q$, keeping Da_A and other conditions constant.

The approach can be extended to other reactive systems by redefining the specific expression for Da_i. The Langmuir Hinshelwood-type kinetic rates and multiple species can be adapted.

Declarations

Author contribution statement

Héctor L. Otálvaro-Marín: Conceived and designed the experiments; Performed the experiments; Analyzed and interpreted the data; Contributed reagents, materials, analysis tools or data; Wrote the paper.

Fiderman Machuca-Martinez: Conceived and designed the experiments; Analyzed and interpreted the data; Contributed reagents, materials, analysis tools or data; Wrote the paper.

Funding statement

This work was supported by Minciencias Colombia (811-2018).

Data availability statement

Data included in article/supp. material/referenced in article.

Declaration of interests statement

The authors declare no conflict of interest.

Additional information

No additional information is available for this paper.

References

[1] J. Fang, J.J. Cambareri, M. Li, N. Saini, I.A. Bolotnov, Interface-resolved simulations of reactor flows, Nucl. Technol. 206 (2020) 133–149.
[2] L.F. Cataneda, F.F. Rivera, T. Pérez, J.L. Nava, Mathematical modeling and simulation of the reaction environment in electrochemical reactors, Curr. Opin. Electrochem. 16 (2019) 75–82.
[3] J.S. Devia-Orjuela, L.A. Betancourt-Buitrago, F. Machuca-Martinez, CFD modeling of a UV-A LED baffled flat-plate photoreactor for environment applications: a mining wastewater case, Environ. Sci. Pollut. Res. 26 (2019) 4510–4520.
[4] H.L. Otálvaro-Marín, M.A. Mueses, F. Machuca-Martínez, Boundary layer of photon absorption applied to heterogeneous photocatalytic solar flat plate reactor design, Int. J. Photoenergy 2014 (2014) 1–8.
[5] H.L. Otálvaro-Marín, M. Angel Mueses, J.C. Crittenden, F. Machuca-Martinez, Solar photoreactor design by the photon path length and optimization of the radiant field in a TiO_2-based CPC reactor, Chem. Eng. J. 315 (2017) 283–295.
[6] J. Colina-Márquez, F. Machuca-Martínez, G. Li Puma, Photocatalytic mineralization of commercial herbicides in a pilot-scale solar CPC reactor: photoreactor modeling and reaction kinetics constants independent of radiation field, Environ. Sci. Technol. 43 (2009) 8953–8960.
[7] S. Malato Rodríguez, J. Blanco Gálvez, M.I. Maldonado Rubio, P. Fernández Ibáñez, D. Alarcón Padilla, M. Collares Pereira, J. Farinha Mendes, J. Correia de Oliveira, Engineering of solar photocatalytic collectors, Sol. Energy 77 (2004) 513–524.
[8] M.D.L.M. Ballari, O.M. Alfano, A.E. Cassano, Mass transfer limitations in slurry photocatalytic reactors: experimental validation, Chem. Eng. Sci. 65 (2010) 4931–4942.
[9] H.L. Otálvaro-Marín, F. González-Caicedo, A. Arce-Sarria, M. Angel, J.C. Crittenden, F. Machuca-Martinez, Scaling-up a heterogeneous H_2O_2/TiO_2/solar-radiation system using the Damköhler number, Chem. Eng. J. 364 (2019) 244–256.
[10] H.L. Otálvaro-Marín, F. Machuca-Martinez, Sizing of reactors by charts of Damköhler's number for solutions of dimensionless design equations, Heliyon 6 (11) (2020) e05386.
[11] K. Alhumaizi, R. Henda, M. Soliman, Numerical analysis of a reaction-diffusion-convection system, Comput. Chem. Eng. 27 (2003) 579–594.
[12] N.A. Gómez Mendoza, I. Dobrosz-Gómez, M.Á. Gómez García, Modeling and simulation of an industrial falling film reactor using the method of lines with adaptive mesh. Study case: industrial sulfonation of tridecylbenzene, Comput. Chem. Eng. 68 (2014) 233–241.
[13] A.M. Wazwaz, The decomposition method applied to systems of partial differential equations and to the reaction-diffusion Brusselator model, Appl. Math. Comput. 110 (2000) 251–264.
[14] G.J. Gassner, A.R. Winters, A novel robust strategy for discontinuous Galerkin methods in computational fluid mechanics: why? when? what? where?, Front. Phys. 8 (2021) 1–24.
[15] Standard Tables for Reference Solar Spectral Irradiances: Direct Normal and Hemispherical on 37° Tilted Surface, ASTM G173 03, ASTM Int., 2012.
[16] G. Eisenberg, Colorimetric determination of hydrogen peroxide, Ind. Eng. Chem., Anal. Ed. 15 (1943) 327–328.
[17] J.F. Barona, D.F. Morales, L.F. González-Bahamón, C. Pulgarín, L.N. Benítez, Shift from heterogeneous to homogeneous catalysis during resorcinol degradation using the solar photo-Fenton process initiated at circumneutral pH, Appl. Catal. B, Environ. 165 (2015) 620–627.
[18] G.H. Meyer, The method of lines (MOL) for the diffusion equation, in: Time-Discrete Method Lines Options Bond, 2015, pp. 57–74.
[19] B.A. Finlayson, The method of weighted residuals and variational principles - with application in fluid mechanics, heat and mass transfer, Math. Sci. Eng. 97 (146) (1972) 412.
[20] M.L. Satuf, R.J. Brandi, A.E. Cassano, O.M. Alfano, Scaling-up of slurry reactors for the photocatalytic degradation of 4-chlorophenol, Catal. Today 129 (2007) 110–117.
[21] D.D. Dionysiou, M.T. Suidan, I. Baudin, J.-M. Laîné, Effect of hydrogen peroxide on the destruction of organic contaminants-synergism and inhibition in a continuous-mode photocatalytic reactor, Appl. Catal. B, Environ. 50 (2004) 259–269.
[22] C.S. Turchi, D.F. Ollis, Photocatalytic degradation of organic water contaminants: mechanisms involving hydroxyl radical attack, J. Catal. 122 (1990) 178–192.

[23] R. Alimoradzadeh, A. Assadi, S. Nasseri, M.R. Mehrasbi, Photocatalytic degradation of 4-chlorophenol by UV/H_2O_2/NiO process in aqueous solution, J. Environ. Health Sci. Eng. 9 (2012) 1–8.
[24] D.G. Blackmond, Kinetic profiling of catalytic organic reactions as a mechanistic tool, J. Am. Chem. Soc. 137 (2015) 10852–10866.
[25] G. Li Puma, V. Puddu, H.K. Tsang, A. Gora, B. Toepfer, Photocatalytic oxidation of multicomponent mixtures of estrogens (estrone (E1), 17β-estradiol (E2), 17α-ethynylestradiol (EE2) and estriol (E3)) under UVA and UVC radiation: photon absorption, quantum yields and rate constants independent of photon absorption, Appl. Catal. B, Environ. 99 (2010) 388–397.
[26] J.C. Crittenden, R.R. Trussell, D.W. Hand, K.j. Howe, G. Tchobanoglous, J.H. Borchardt, MWH's Water Treatment Principles and Design, third edition, John Wiley and Sons, Inc, Hoboken, New Jersey, 2012.
[27] M.I. Cabrera, O.M. Alfano, A.E. Cassano, Absorption and scattering coefficients of titanium dioxide particulate suspensions in water, J. Phys. Chem. 100 (1996) 20043–20050.
[28] S. Yang, C. Sun, X. Li, Z. Gong, X. Quan, Enhanced photocatalytic activity for titanium dioxide by co-modifying with silica and fluorine, J. Hazard. Mater. 175 (2010) 258–266.
[29] R. Acosta-Herazo, J. Monterroza-Romero, M.Á. Mueses, F. Machuca-Martínez, G. Li Puma, Coupling the six flux absorption-scattering model to the Henyey-Greenstein scattering phase function: evaluation and optimization of radiation absorption in solar heterogeneous photoreactors, Chem. Eng. J. 302 (2016) 86–96.
[30] G. Han, Y. Sun, Visible-light-driven organic transformations on semiconductors, Mater. Today Phys. 16 (2020) 100297.
[31] J. Diaz-Angulo, A. Arce-Sarria, M. Mueses, A. Hernandez-Ramirez, F. Machuca-Martinez, Analysis of two dye-sensitized methods for improving the sunlight absorption of TiO_2 using CPC photoreactor at pilot scale, Mater. Sci. Semicond. Process. 103 (2019) 104640.
[32] G. Li Puma, P.L. Yue, A novel fountain photocatalytic reactor: model development and experimental validation, Chem. Eng. Sci. 56 (2001) 2733–2744.
[33] K.S. Ochoa-Gutiérrez, E. Tabares-Aguilar, M.Á. Mueses, F. Machuca-Martínez, G. Li Puma, A novel prototype offset multi tubular photoreactor (OMTP) for solar photocatalytic degradation of water contaminants, Chem. Eng. J. 341 (2018) 628–638.
[34] N.M. Reis, G. Li Puma, A novel microfluidic approach for extremely fast and efficient photochemical transformations in fluoropolymer microcapillary films, Chem. Commun. 51 (2015) 8414–8417.
[35] M.D.L.M. Ballari, R.J. Brandi, O.M. Alfano, A.E. Cassano, Mass transfer limitations in photocatalytic reactors employing titanium dioxide suspensions I. Concentration profiles in the bulk, Chem. Eng. J. 136 (2008) 50–65.